



Crystal Structure Of Cr³⁺ Ions Substituted Co-Ferrite Nanoparticles

S. R. Bainade*¹, C. M. Kale², G. R. Jadhav¹, M. C. Sable¹

¹Department of Physics, Jijamata Mahavidyalaya, Buldhana, Maharashtra, India

²Department of Physics, Indraraj Arts, Commerce and Science College, Sillod-Aurangabad, Maharashtra, India

ABSTRACT

A series of polycrystalline spinel ferrite having the chemical formula $\text{CoCr}_x\text{Fe}_{2-x}\text{O}_4$ ($x = 0.0, 0.2, 0.4, 0.6, 0.8,$ and 1.0) were synthesized by using sol-gel auto combustion method and studied by using X-ray diffraction (XRD) measurements. The XRD analysis reveals single phase cubic spinel structure of synthesized samples. The particle size of was found by XRD and scanning electron microscopy (SEM) technique confirms the nanocrystalline nature of the samples.

Keywords: Sol-gel, X-ray diffraction, structural properties

I. INTRODUCTION

Ferrite materials are metal oxides have high electrical resistivity, low eddy current losses and convincingly low costs coupled with their potential microwave applications such as circulators, isolators and phase shifters. Now a day nanosized ferrite materials have been widely used to prepare many electromagnetic devices such as inductors, converters, phase shifters and electromagnetic wave absorbers [1].

On the basis of crystal structure, ferrites are grouped into three important classes, namely spinel ferrite, garnet and hexa-ferrite [2]. Spinel ferrites are represented by the formula AFe_2O_4 , where A is a divalent metal ion. The crystal structure of ferrite consists of two interstitial sites, tetrahedral (A) and octahedral (B) sites, in which cations are occupied. So that it is essential to know the crystal structural of ferrite material. Ferrites made from nanoparticles can show different properties unlike those observed in bulk material. The structural properties of these materials can be attributed to the small size, a large surface to volume ratio, cation distribution, concentration of localized electric charge carriers, and stoichiometry.

The identification of new materials with improvement in properties or new processing techniques to improve the performance of existing materials, along with the economical advantages, is always a matter of interest to researchers. The fabrication of spinel ferrites nanoparticles has been the subject of intense research interest due to their excellent magnetic, electrical and dielectric properties [3].

According to literature, several researchers focused only few properties of ferrite material, however the structural, electrical and dielectric properties of Cr³⁺ substituted cobalt ferrite has not been investigated together in detail by the researchers [4-6].

Cr³⁺ with antiferromagnetic nature is known for achieving good control over electric as well as dielectric parameters in developing technologically important materials. The substitution of Cr³⁺ ions for Fe³⁺ ions will improve the properties marked similarly to that of nonmagnetic substitution. In the present study, we synthesized $\text{CoCr}_x\text{Fe}_{2-x}\text{O}_4$ ($x = 0.0, 0.2, 0.4, 0.6, 0.8,$ and 1.0) ferrite nanoparticles by using the sol-gel auto combustion method and investigated the consequent

changes on crystal structure of the Cr³⁺ substituted cobalt ferrite.

II. EXPERIMENTAL

For the synthesis of CoCr_xFe_{2-x}O₄ (where x = 0.0 to 1.0 in the step of 0.2) by sol-gel auto combustion method, calculated quantities of metal nitrates were dissolved together in a 100ml of deionised distilled water to get clear solution. An aqueous solution of citric acid then added to the metal nitrate solution. The molar ratio (citric acid to the total moles of nitrate ions) was adjusted to 1:3. A small amount of liquid ammonia (NH₃) was added drop wise into the solution so as to maintain pH value to about 7. A continuous stirring and heating the solution at 90°C on hot plate with magnetic stirrer until it becomes a viscous gel. The process of mixing till continued to burn the material in the powder form. The complete process is shown with in the flow chart Figure 1. The powder was annealed in air at temperature 500°C for 6h with heating rate 50°C per min to obtain a spinel phase. The final product is then grinded and subjected to further study.

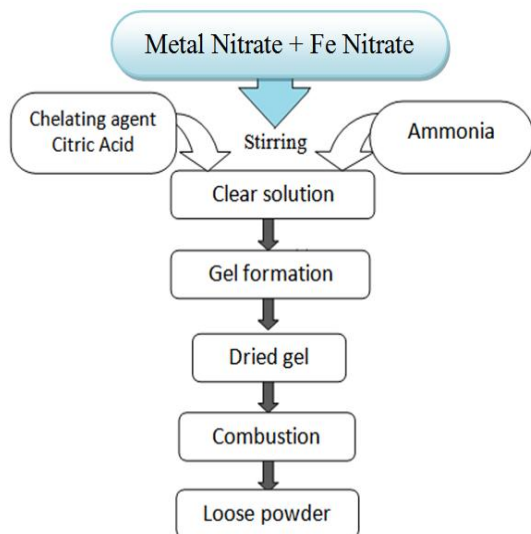


Figure 1. Flow chart shows the stages involved in preparation of spinel ferrite by sol-gel auto combustion method

III. RESULT AND DISCUSSION

3.1. Structural analysis:

3.1.1. X-ray diffraction and lattice constant

The X-ray diffraction (XRD) patterns of the typical samples (x=0.6, 0.8, 1.0) of CoCr_xFe_{2-x}O₄ nanoferrite system were shown in Figure 2.

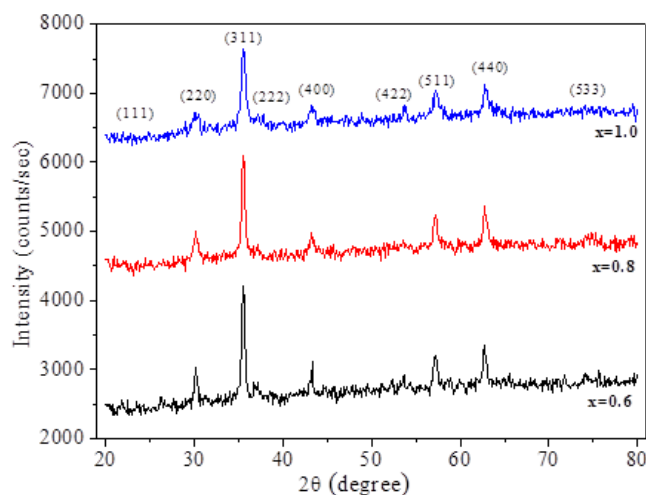


Figure 2. Typical XRD patterns for x= (0.6, 0.8, 1.0) of CoCr_xFe_{2-x}O₄ nanoferrite system

The XRD patterns of all the Cr substituted cobalt ferrites shows single phase cubic spinel structure. The XRD shows the reflection such as (111), (220), (311), (222), (400), (422), (511), (440), (533) which belongs to cubic spinel ferrite. All the Bragg reflections peaks are allowed peaks have been indexed without any impurity peaks. The strongest reflection has come from (311) plane that indicates spinel phase.

Lattice constant (a) of all composition was calculated by using the formula,

$$a = d\sqrt{N} \text{ \AA}$$

where $N = h^2 + k^2 + l^2$ and 'd' is the interplaner spacing.

The variation of lattice parameter with Cr³⁺ compositions lies in between 8.3939 Å to 8.3371 Å is listed in Table 1. The lattice parameter was found to decrease linearly with increasing Cr³⁺ content x. This linear variation indicates that the Co-Cr ferrite system obeys Vegard's law [7]. A similar behavior of lattice constant with dopant concentration was observed by several investigators in various ferrite systems. The decrease in lattice parameter with increase in Cr³⁺ content can be explained on the basis of relative ionic radii of Cr³⁺ (0.63 Å) and Fe³⁺ (0.64 Å) ions. Calculated lattice parameter for Cobalt ferrite (CoFe₂O₄) was in good agreement with the standard value (8.391 Å) reported from ICSD data. As Cr³⁺ ions have small ionic radii than that of Fe³⁺ a partial replacement of Fe³⁺ ions by Cr³⁺ ions results in a decrease in lattice parameter.

There exists a correlation between the ionic radius and the lattice constant, the increase of the lattice constant is proportional to the increase of the ionic radius [8, 9].

3.1.2. Particle size

Using the literature sol-gel method is the only method which has resulted in Co-Cr ferrites with such a very small particle size. The average particle size (t) of all sample compositions has been calculated from full width at half maximum (FWHM) of broadening of the most intense peaks (311) using the following Debye-Scherrer formula [10].

$$t = \frac{k\lambda}{\beta \cos \theta} \text{ \AA}$$

where, λ is the X-ray wavelength ($=1.5405\text{\AA}$) of radiation, k is the shape factor with typical value 0.94, β is the line broadening at FWHM of the diffraction peak and θ is the diffraction angle in radian.

The values of particle size obtained from XRD data and SEM (Table 1) are in response to the increase in Cr^{3+} ions substitution. The average particle sizes is found in the range ~ 14 to 28 nm which are close to the results obtained from SEM images and good agreement with report of Sonal Singhal et.al. [11]

Table 1. Lattice constant, particle size, of $\text{CoCr}_x\text{Fe}_{2-x}\text{O}_4$ nanoferrite system

Ferrite composition	Lattice constant 'a' (Å)	Particle size 't' (nm)	
		XRD	SEM
CoFe_2O_4	8.3939	27.80	27
$\text{CoCr}_{0.2}\text{Fe}_{1.8}\text{O}_4$	8.3812	20.85	20
$\text{CoCr}_{0.4}\text{Fe}_{1.6}\text{O}_4$	8.3722	16.68	18
$\text{CoCr}_{0.6}\text{Fe}_{1.4}\text{O}_4$	8.3604	20.85	20
$\text{CoCr}_{0.8}\text{Fe}_{1.2}\text{O}_4$	8.3485	20.85	20
$\text{CoCr}_{1.0}\text{Fe}_{1.0}\text{O}_4$	8.3371	13.90	14

3.1.3. Bond length

Bond lengths R_A and R_B are the shortest distance between A-site and B-site cations with the oxygen ion respectively. The variation of the bond length R_A and R_B of $\text{CoCr}_x\text{Fe}_{2-x}\text{O}_4$ nanoferrite system calculated by the equation [12] and listed in Table 2.

The values R_B are greater than R_A indicates that the B-site cations Co^{2+} are closer to oxygen O^{2-} ions exert more attractive force. The value of bond lengths R_A and R_B decreases from 1.904 to 1.892 Å and 2.048 to 2.036 Å respectively as Cr^{3+} ion content increases. The value of B-site Cr^{3+} ions is greater than A-site Co^{2+} ions. This may be explained on the basis of difference in ionic radii of constituent ions Cr^{3+} (0.63 Å) and Co^{2+} (0.82 Å). The behavior of bond lengths is attributed to variation of lattice constant with Cr content x [13].

3.1.4. Tetrahedral and octahedral bond edges

The bond length of tetrahedral (A) site ' d_{AX} ' and octahedral [B] site ' d_{BX} ', tetrahedral edge ' d_{AXE} ', shared octahedral edge ' d_{BXE} ' and unshared octahedral edge ' d_{BXEU} ' of $\text{CoCr}_x\text{Fe}_{2-x}\text{O}_4$ nanoferrite system were calculated by using the values of lattice constant ' a ' and oxygen positional parameter ' u ', in the standard equations.

The calculated values are depicted in Figure 3. The Figure 3 indicates that the tetrahedral bond length d_{AX} and octahedral bond length d_{BX} decrease as Cr^{3+} content x increases. Also shows that the tetrahedral edge ' d_{AXE} ', ' d_{BXE} ' unshared octahedral edge ' d_{BXEU} ' does not vary much with composition while shared octahedral edge ' d_{BXE} ' decreases [14]. The observed behavior is attributed to decrease in the lattice constant with the Cr content (x) due to smaller ionic radii of Cr^{3+} ions.

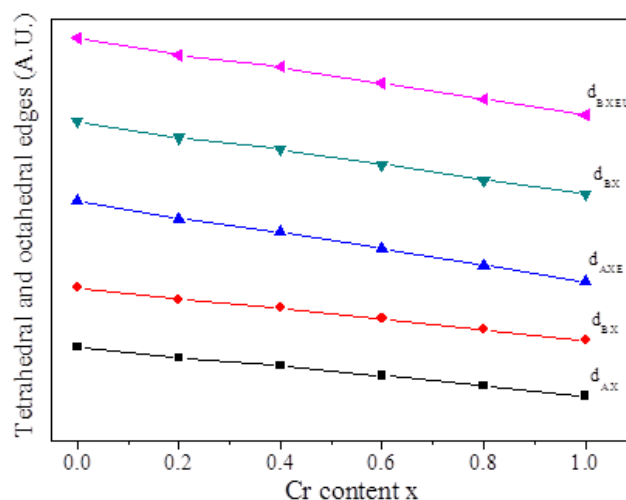


Figure 3. Tetrahedral and octahedral bond edges with Cr content x of $\text{CoCr}_x\text{Fe}_{2-x}\text{O}_4$ nanoferrite system

3.1.5 Scanning electron micrographs (SEM) analysis

SEM was used to investigate the change of microstructures of the synthesized $\text{CoCr}_x\text{Fe}_{2-x}\text{O}_4$ nanoferrite powder samples with Cr content x . The prepared ferrite powders were recorded by using scanning electron microscope (JSM-6360 model) at Dept. of Physics, SPPU, Pune. The micrograph of the recorded typical sample ($x=0.8$) is as shown in Figure 4.



Figure 4. Typical SEM image of $\text{CoCr}_x\text{Fe}_{2-x}\text{O}_4$ nanoferrite system

From the SEM images, it is observed that the prepared samples are porous in nature. It should also be noted that, though sintering temperature 500°C is responsible for small amount of pores in SEM images reveals that the sintering is done in a satisfactory manner without loss of Cr ions in all samples. The effect of increasing Cr^{3+} content on the investigated samples is the enhancement of the grain growth as seen from the SEM [15]. Uniform grains are progressively increased with increasing Cr^{3+} content x and the ferrite samples exhibit an aggregated continuous grain growth. The particle size determined from SEM images is in the range from 14 to 27nm by linear intercept method [16] and the values are given in Table 1.

IV. CONCLUSION

The substitution of Cr^{3+} ions in Co-ferrite has been successfully investigated by sol-gel auto combustion method. Powder XRD, SEM data indicate clearly the information of ultrafine single phase cubic spinel structure of synthesized Co-Cr ferrite material. The particle size obtain in between 14 to 28 nm. Bond length, tetrahedral and octahedral bond edges are directly depends on lattice constant.

V. REFERENCES

- [1]. V. G. Harris, A. Geiler, Y. J. Chen, S. D. Yoon, M. Z. Wu, A. Yang, Z. H. Chen, P. He, P. V. Parimi, X. Zuo, C. E. Patton, M. Abe, O. Acher and C. Vittoria, *J. Magn. Magn. Mater.*, 321, 2035 (2009)
- [2]. G.P. Rodrigue, *IEEE Transactions on Microwave Theory and Techniques* 11 (1969) 351
- [3]. Y. P. Fu, S. H. Hu, *Ceram. Int.*, 36, 1311 (2010)
- [4]. Dana Gingasu, Lucian Diamandescu, Ioana Mindru, Gabriela Marinescu, Daniela C. Culita, Jose Maria Calderon-Moreno, Silviu Preda, Cristina Bartha, *Luminita Patron, Croat. Chem. Acta* 2015, 88(4) 445–451
- [5]. Mamilla Lakshmi, Katrapally Vijaya Kumar Krishnan Thyagarajan, *Advances in Nanoparticles*, 2016, 5, 103-113
- [6]. M. Raghassudha, D. Ravinder, P. Veerasomaiah, *Nanoscience and Nanotechnology* 2013, 3(5),105-114
- [7]. Kumar P., Mishra P., Sahu S. K. *Inter. J. Scien. Eng. Res.* 2(8) (2011)
- [8]. S. R. Bainade, C. M. Kale, M. C. Sable, *J. Supercond. Nov. Magn*, July 2017
- [9]. M.Leszczynski, E. Litwin-Staszewska, T. Suski, *Acta Physica Polonica A*, 88 (1995)
- [10]. Cullity B.D. , Stock S.R. 2001, *Elements of X-ray diffraction* (New York, Prentice Hall) P-154
- [11]. Sonal Singhal, Sheenu Jauhar, Kailas Chandra, Sandeep Bansal. *Bull. Mater. Sci.* Vol.36 No.1 (2013) pp-107-114
- [12]. Standley K. J., 1972, *Oxide Magnetic Material*, Oxford, U. K. Clarendon
- [13]. Zakaria, A.K.M., Nesa, F., Khan, M.S., Yunus, S.M., Khan, N.I., Saha, D.K. and Eriksson, S.G., *Journal of Bangladesh Academy of Sciences*, 39 (2015) 1
- [14]. R. K. Sharma, V. Sebastian, N. Lakshmi, K. Venugopalan, V. R. Reddy, A. Gupta, *Phy. Rev. B* 75 (2007) 144419
- [15]. C.O. Augustin, L.K. Srinivasan, P. Kamaraj and A. Mani, *J.Mater. Sci. Technol.*12, P-417-420 (1996)
- [16]. Wurst J.C., Nelson J. A. (1972) *Am. Ceram. Soc. Bull.*, 55,109